THE EUROPEAN
PHYSICAL JOURNAL C

CrossMark

Transverse-target-spin asymmetry in exclusive ω-meson electroproduction

HERMES Collaboration

A. Airapetian[15,18], N. Akopov[29], Z. Akopov[7], E. C. Aschenauer[8], W. Augustyniak[28], A. Avetissian[29], S. Belostotski[21], H. P. Blok[20,27], A. Borissov[7], V. Bryzgalov[22], G. P. Capitani[13], G. Ciullo[11,12], M. Contalbrigo[11], P. F. Dalpiaz[11,12], W. Deconinck[7], R. De Leo[2], E. De Sanctis[13], M. Diefenthaler[10,17], P. Di Nezza[13], M. Düren[15], G. Elbakian[29], F. Ellinghaus[6], L. Felawka[25], S. Frullani[23,24], D. Gabbert[8], G. Gapienko[22], V. Gapienko[22], V. Gharibyan[29], F. Giordano[11,12,17], S. Gliske[18], D. Hasch[13], M. Hoek[16], Y. Holler[7], A. Ivanilov[22], H. E. Jackson[1], S. Joosten[14], R. Kaiser[16], G. Karyan[29], T. Keri[15], E. Kinney[6], A. Kisselev[21], V. Korotkov[22], V. Kozlov[19], V. G. Krivokhijine[9], L. Lagamba[2], L. Lapikás[20], I. Lehmann[16], P. Lenisa[11,12], W. Lorenzon[18], B.-Q. Ma[3], S. I. Manaenkov[21], Y. Mao[3], B. Marianski[28], H. Marukyan[29], Y. Miyachi[26], A. Movsisyan[11,29], V. Muccifora[13], Y. Naryshkin[21], A. Nass[10], M. Negodaev[8], W.-D. Nowak[8], L. L. Pappalardo[11,12], R. Perez-Benito[15], A. Petrosyan[29], P. E. Reimer[1], A. R. Reolon[13], C. Riedl[8,17], K. Rith[10], G. Rosner[16], A. Rostomyan[7], J. Rubin[17,18], D. Ryckbosch[14], Y. Salomatin[22], G. Schnell[4,5,14,a], B. Seitz[16], T.-A. Shibata[26], M. Statera[11,12], E. Steffens[10], J. J. M. Steijger[20], F. Stinzing[10], S. Taroian[29], A. Terkulov[19], R. Truty[17], A. Trzcinski[28], M. Tytgat[14], Y. Van Haarlem[14], C. Van Hulse[4,14], V. Vikhrov[21], I. Vilardi[2], C. Vogel[10], S. Wang[3], S. Yaschenko[7,10], S. Yen[25], B. Zihlmann[7], P. Zupranski[28]

[1] Physics Division, Argonne National Laboratory, Argonne, IL 60439-4843, USA
[2] Sezione di Bari, Istituto Nazionale di Fisica Nucleare, 70124 Bari, Italy
[3] School of Physics, Peking University, Beijing 100871, China
[4] Department of Theoretical Physics, University of the Basque Country UPV/EHU, 48080 Bilbao, Spain
[5] IKERBASQUE, Basque Foundation for Science, 48013 Bilbao, Spain
[6] Nuclear Physics Laboratory, University of Colorado, Boulder, CO 80309-0390, USA
[7] DESY, 22603 Hamburg, Germany
[8] DESY, 15738 Zeuthen, Germany
[9] Joint Institute for Nuclear Research, 141980 Dubna, Russia
[10] Physikalisches Institut, Universität Erlangen-Nürnberg, 91058 Erlangen, Germany
[11] Sezione di Ferrara, Istituto Nazionale di Fisica Nucleare, 44122 Ferrara, Italy
[12] Dipartimento di Fisica e Scienze della Terra, Università di Ferrara, 44122 Ferrara, Italy
[13] Istituto Nazionale di Fisica Nucleare, Laboratori Nazionali di Frascati, 00044 Frascati, Italy
[14] Department of Physics and Astronomy, Ghent University, 9000 Gent, Belgium
[15] II. Physikalisches Institut, Justus-Liebig Universität Gießen, 35392 Gießen, Germany
[16] SUPA, School of Physics and Astronomy, University of Glasgow, Glasgow G12 8QQ, UK
[17] Department of Physics, University of Illinois, Urbana, IL 61801-3080, USA
[18] Randall Laboratory of Physics, University of Michigan, Ann Arbor, MI 48109-1040, USA
[19] Lebedev Physical Institute, 117924 Moscow, Russia
[20] National Institute for Subatomic Physics (Nikhef), 1009 DB Amsterdam, The Netherlands
[21] B.P. Konstantinov Petersburg Nuclear Physics Institute, Gatchina, 188300 Leningrad Region, Russia
[22] Institute for High Energy Physics, Protvino, 142281 Moscow Region, Russia
[23] Gruppo Collegato Sanità, Sezione di Roma, Istituto Nazionale di Fisica Nucleare, 00161 Rome, Italy
[24] Istituto Superiore di Sanità, 00161 Rome, Italy
[25] TRIUMF, Vancouver, BC V6T 2A3, Canada
[26] Department of Physics, Tokyo Institute of Technology, Tokyo 152, Japan
[27] Department of Physics and Astronomy, VU University, 1081 HV Amsterdam, The Netherlands
[28] National Centre for Nuclear Research, 00-689 Warsaw, Poland
[29] Yerevan Physics Institute, 375036 Yerevan, Armenia

F. Stinzing: Deceased.

[a] e-mail: gunar.schnell@desy.de

Abstract Hard exclusive electroproduction of ω mesons is studied with the HERMES spectrometer at the DESY laboratory by scattering 27.6 GeV positron and electron beams

Springer

off a transversely polarized hydrogen target. The amplitudes of five azimuthal modulations of the single-spin asymmetry of the cross section with respect to the transverse proton polarization are measured. They are determined in the entire kinematic region as well as for two bins in photon virtuality and momentum transfer to the nucleon. Also, a separation of asymmetry amplitudes into longitudinal and transverse components is done. These results are compared to a phenomenological model that includes the pion pole contribution. Within this model, the data favor a positive $\pi\omega$ transition form factor.

1 Introduction

In the framework of quantum chromodynamics (QCD), hard exclusive meson leptoproduction on a longitudinally or transversely polarized proton target provides important information about the spin structure of the nucleon. The process amplitude is a convolution of the lepton–quark hard-scattering subprocess amplitude with soft hadronic matrix elements describing the structure of the nucleon and that of the meson. Here, factorization is proven rigorously only if the lepton–quark interaction is mediated by a longitudinally polarized virtual photon [1,2]. The soft hadronic matrix elements describing the nucleon contain generalized parton distributions (GPDs) to parametrize its partonic structure. Hard exclusive production of vector mesons is described by GPDs H^f and E^f, where f denotes a quark flavor or a gluon. These "unpolarized", i.e., parton–helicity–nonflip distributions describe the photon–parton interaction with conservation and flip of nucleon helicity, respectively. Both are of special interest, as they are related to the total angular momentum of partons, J^f [3]. The GPDs H^f are well constrained by existing experimental data. The GPDs E^u and E^d for up and down quarks, respectively, are partially constrained by nucleon form-factor data [4], while experimental information on sea-quark GPD E^{sea} and gluon GPD E^g is scarce. For a recent review on the status of GPD determinations, see Ref. [5]. In contrast to leptoproduction of vector mesons with an unpolarized target, which is mainly sensitive to GPDs H^f, vector-meson leptoproduction off a transversely polarized nucleon is sensitive to the interference between two amplitudes containing H^f and E^f, respectively, and thus opens access to E^f.

For a transversely polarized virtual photon mediating the lepton–quark interaction, there exists no rigorous proof of collinear factorization. In the QCD-inspired phenomenological "GK" model [6–8] however, factorization is also assumed for the transverse amplitudes. In this so-called modified perturbative approach [9], infrared singularities occurring in these amplitudes are regularized by quark transverse momenta in the subprocess, while the partons are still emitted and reabsorbed collinearly by the nucleon. By using the

quark transverse momenta in the subprocess, the transverse size of the meson is effectively taken into account. Using this approach, the GK model describes cross sections, spin density matrix elements (SDMEs), and spin asymmetries in exclusive vector-meson production for values of Bjorken-x below 0.2 [6–8]. The GPDs parametrized in the GK model were used in calculations of deeply virtual Compton scattering (DVCS) amplitudes, which led to good agreement with most DVCS measurements over a wide kinematic range [10]. In the most recent version of the model, the $\gamma^*\pi\omega$ vertex function in the one-pion-exchange contribution is identified with the $\pi\omega$ transition form factor [11]. Its magnitude is determined in a model-dependent way, while its unknown sign may be determined from comparisons with experimental data on spin asymmetries in hard exclusive leptoproduction.

Measurements of hard-exclusive production of various types of mesons are complementary to DVCS, as they allow access to various flavor combinations of GPDs. Previous HERMES publications on measurements of azimuthal transverse-target-spin asymmetries include results on exclusive production of ρ^0 [12] and π^+ mesons [13] as well as on DVCS [14].

In the present paper, the azimuthal modulations of the transverse-target-spin asymmetry in the cross section of exclusive electroproduction of ω mesons are studied. The available data allow for an estimation of the kinematic dependence of the measured asymmetry amplitudes on photon virtuality and four-momentum transfer to the nucleon. The measured asymmetry amplitudes are compared to the most recent calculations of the GK model using either possible sign of the $\pi\omega$ transition form factor.

2 Data collection and process identification

The data were accumulated with the HERMES forward spectrometer [15] during the running period 2002–2005. The 27.6 GeV positron (electron) beam was scattered off a transversely polarized hydrogen target, with the average magnitude P_T of the proton-polarization component $\mathbf{P_T}$ perpendicular to the beam direction being equal to 0.72. The lepton beam was longitudinally polarized, and in the analysis the data set is beam-helicity balanced. The ω meson is produced in the reaction

$$e + p \rightarrow e + p + \omega, \tag{1}$$

with a branching ratio $Br = 89.1\%$ for the ω decay

$$\omega \rightarrow \pi^+ + \pi^- + \pi^0, \quad \pi^0 \rightarrow 2\gamma. \tag{2}$$

The same requirements to select exclusively produced ω mesons as in Ref. [16] are applied. The candidate events for exclusive ω-meson production are required to have exactly three charged tracks, i.e., the scattered lepton and
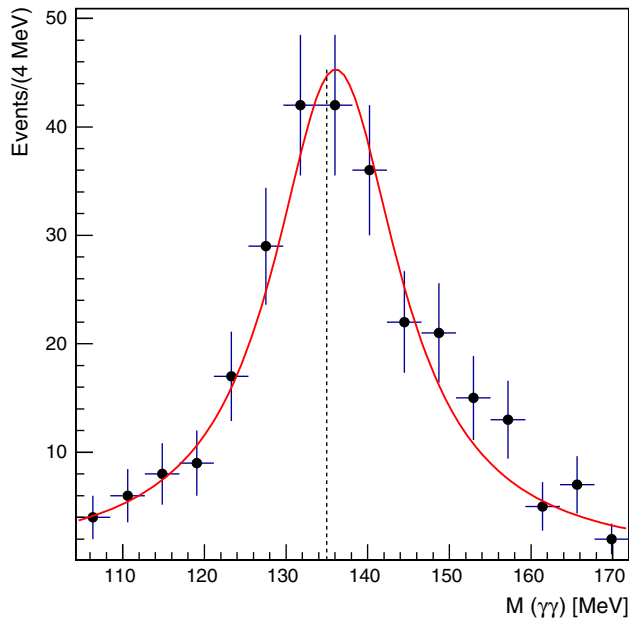
Fig. 1 Two-photon invariant-mass distribution after application of all criteria to select exclusively produced ω mesons. The Breit–Wigner fit to the mass distribution is shown as a *continuous line* and the *vertical dashed line* indicates the PDG value of the π^0 mass [17]
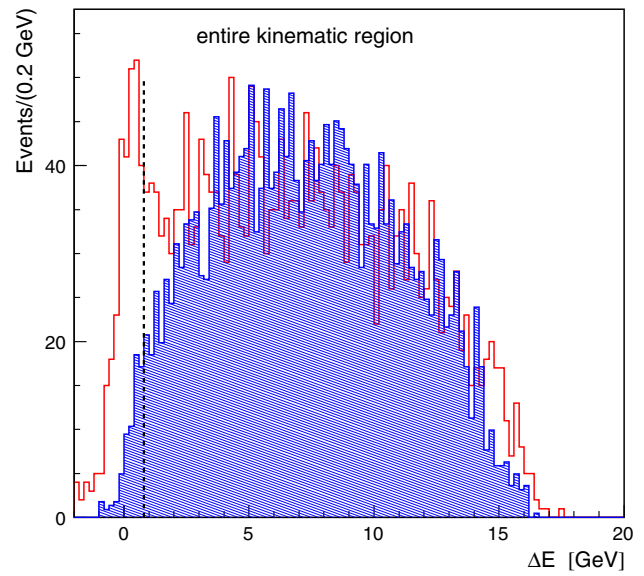

Fig. 2 Missing-energy distribution for exclusive ω-meson production. The *unshaded histogram* shows experimental data, while the *shaded area* shows the distribution obtained from a PYTHIA simulation of the SIDIS background. The *vertical dashed line* denotes the upper limit of the exclusive region

two oppositely charged pions, and at least two clusters in the calorimeter not associated with a charged track. The π^0 meson is reconstructed from two photon clusters with an invariant mass $M(\gamma\gamma)$ in the interval 0.11 GeV $< M(\gamma\gamma) < 0.16$ GeV. Its distribution is shown in Fig. 1, where the fit with a Breit–Wigner function yields 136.1 ± 0.8 MeV (19 ± 2 MeV) for the mass (width). The charged hadrons and leptons are identified through the combined responses of four particle-identification detectors [15]. The three-pion invariant mass is calculated as $M(\pi^+\pi^-\pi^0) = \sqrt{(p_{\pi^+} + p_{\pi^-} + p_{\pi^0})^2}$, where p_π are the four-momenta of the charged and neutral pions. Events containing ω mesons are selected through the requirement 0.71 GeV $< M(\pi^+\pi^-\pi^0) < 0.87$ GeV.

Further event-selection requirements are the following:

(i) $1.0\,\mathrm{GeV}^2 < Q^2 < 10.0\,\mathrm{GeV}^2$, where Q^2 represents the negative square of the virtual-photon four-momentum. The lower value is applied in order to facilitate the application of perturbative QCD, while the upper value delimits the measured phase space;

(ii) $-t' < 0.2\,\mathrm{GeV}^2$ in order to improve exclusivity, where $t' = t - t_{min}$, t is the squared four-momentum transfer to the nucleon and $-t_{min}$ represents the smallest kinematically allowed value of $-t$ at fixed virtual-photon energy and Q^2;

(iii) $W > 3$ GeV in order to be outside of the resonance region and $W < 6.3$ GeV in order to clearly delimit the

kinematic phase space, where W is the invariant mass of the photon-nucleon system;

(iv) the scattered-lepton energy lies above 3.5 GeV in order to avoid a bias originating from the trigger.

In order to isolate exclusive production, the energy not accounted for by the leptons and the three pions must be zero within the experimental resolution. We require the missing energy to be in the interval -1.0 GeV $< \Delta E < 0.8$ GeV, which is referred to as "exclusive region" in the following. Here, the missing energy is calculated as $\Delta E = \frac{M_X^2 - M_p^2}{2M_p}$, with M_p being the proton mass and $M_X^2 = (p + q - p_{\pi^+} - p_{\pi^-} - p_{\pi^0})^2$ the missing-mass squared, where p and q are the four-momenta of target nucleon and virtual photon, respectively. The distribution of the missing energy ΔE is shown in Fig. 2. It exhibits a clearly visible exclusive peak centered about $\Delta E = 0$. The shaded area represents semi-inclusive deep-inelastic scattering (SIDIS) background events obtained from a PYTHIA [18] Monte-Carlo simulation that is normalized to the data in the region 2 GeV $< \Delta E < 20$ GeV. The simulation is used to determine the fraction of background under the exclusive peak. This fraction is calculated as the ratio of the number of background events to the total number of events and amounts to about 21 %.

After application of all these constraints, the sample contains 279 exclusively produced ω mesons. This data sample is referred to in the following as data in the "entire kinematic
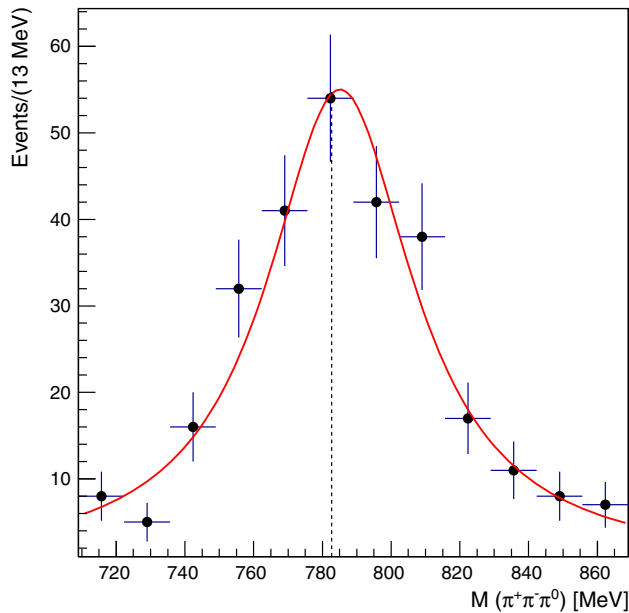
Fig. 3 The $\pi^+\pi^-\pi^0$ invariant-mass distribution after application of all criteria to select exclusively produced ω mesons. The Breit–Wigner fit to the mass distribution is shown as a *continuous line* and the *vertical dashed line* indicates the PDG value of the ω mass [17]

region". The $\pi^+\pi^-\pi^0$ invariant-mass distribution for this data sample is shown in Fig. 3. A Breit–Wigner fit yields 785 ± 2 MeV (52 ± 5 MeV) for the mass (width).

3 Extraction of the asymmetry amplitudes

The cross section for hard exclusive leptoproduction of a vector meson on a transversely polarized proton target, written in terms of polarized photo-absorption cross sections and interference terms, is given by Eq. (34) in Ref. [19]. In this equation, the transverse-target-spin asymmetry A_{UT} is decomposed into a Fourier series of terms involving $\sin(m\phi \pm \phi_S)$, with $m = 0, \ldots, 3$. The angles ϕ and ϕ_S are the azimuthal angles of the ω-production plane and of the component $\mathbf{S}_\perp$ of the transverse nucleon polarization vector that is orthogonal to the virtual-photon direction. They are measured around the virtual-photon direction and with respect to the lepton-scattering plane (see Fig. 4). These definitions are in accordance with the Trento Conventions [20]. For the HERMES kinematics and acceptance in exclusive ω production, $\sin\theta_{\gamma^*} < 0.1$ and $\cos\theta_{\gamma^*} > 0.99$, which can be approximated by $\sin\theta_{\gamma^*} \approx 0$ and $\cos\theta_{\gamma^*} \approx 1$. Here, θ_{γ^*} is the angle between the lepton-beam and virtual-photon directions.

In this approximation, the angular-dependent part of Eq. (34) in Ref. [19] for an unpolarized beam reads:

$$\mathcal{W}(\phi, \phi_S) = 1 + A_{UU}^{\cos(\phi)} \cos(\phi) + A_{UU}^{\cos(2\phi)} \cos(2\phi)$$
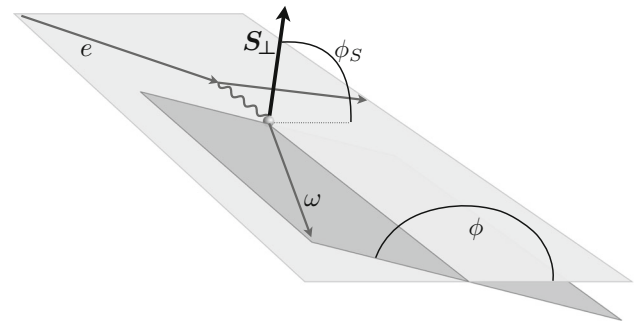$$+ S_\perp [A_{UT}^{\sin(\phi+\phi_S)} \sin(\phi + \phi_S)$$

Fig. 4 Lepton-scattering and ω-production planes together with the azimuthal angles ϕ and ϕ_S

$$+ A_{UT}^{\sin(\phi-\phi_S)} \sin(\phi - \phi_S)$$
$$+ A_{UT}^{\sin(\phi_S)} \sin(\phi_S)$$
$$+ A_{UT}^{\sin(2\phi-\phi_S)} \sin(2\phi - \phi_S)$$
$$+ A_{UT}^{\sin(3\phi-\phi_S)} \sin(3\phi - \phi_S)], \tag{3}$$

where $S_\perp = |\mathbf{S}_\perp|$. Here, A_{UU} and A_{UT} denote the amplitudes of the corresponding cosine and sine modulations as given in their superscripts. The first letter in the subscript denotes unpolarized beam and the second letter U (T) denotes unpolarized (transversely polarized) target. The above approximation in conjunction with the additional factor $\epsilon/2 \approx 0.4$, where ϵ is the ratio of fluxes of longitudinal and transverse virtual photons, allows one to neglect the contribution of the $\sin(2\phi + \phi_S)$ modulation, appearing in Eq. (34) of Ref. [19]. This approximation also makes the angular dependence of $S_\perp$ disappear (see Eq. (8) of Ref. [19]), and $S_\perp \simeq P_T = 0.72$ is used in the following. Note that the modulation $\sin(\phi - \phi_S)$ is the only one that appears at leading twist.

For exclusive production of ω mesons decaying into three pions, the angular distribution of the latter can be decomposed into parts corresponding to longitudinally (L) and transversely (T) polarized ω mesons:

$$\mathcal{W}(\phi, \phi_S, \theta) = \frac{3}{2} r_{00}^{04} \cos^2(\theta) \, w_L(\phi, \phi_S)$$
$$+ \frac{3}{4} (1 - r_{00}^{04}) \sin^2(\theta) \, w_T(\phi, \phi_S). \tag{4}$$

Here, θ is the polar angle of the unit vector normal to the ω decay plane in the ω-meson rest frame, with the z-axis aligned opposite to the outgoing nucleon momentum [16]. The pre-factors r_{00}^{04} and $(1 - r_{00}^{04})$ represent the fractional contribution to the full cross section by longitudinally and transversely polarized ω mesons, respectively [16]. The first (second) term on the right-hand side of Eq. (4) represents the angular distribution of the longitudinally (transversely) polarized ω mesons, with

$$w_L(\phi, \phi_S) = 1 + A_{UU,L}(\phi) + S_\perp A_{UT,L}(\phi, \phi_S),$$
$$w_T(\phi, \phi_S) = 1 + A_{UU,T}(\phi) + S_\perp A_{UT,T}(\phi, \phi_S). \tag{5}$$

The functions $A_{UU,K}(\phi)$ and $A_{UT,K}(\phi, \phi_S)$, with $K = L$ and $K = T$ denoting longitudinal-separated and transverse-separated contributions, respectively, are decomposed into a Fourier series in complete analogy to Eq. (3).

The function $\mathcal{W}(\phi, \phi_S)$ is fitted to the experimental angular distribution using an unbinned maximum likelihood method. Here and in the following, the angle θ has to be added to the argument list of the function $\mathcal{W}$, when applicable. The function to be minimized is the negative of the logarithm of the likelihood function:

$$-\ln L(\mathcal{R}) = -\sum_{i=1}^{N} \ln \frac{\mathcal{W}(\mathcal{R}; \phi^i, \phi_S^i)}{\widetilde{\mathcal{N}}(\mathcal{R})}. \tag{6}$$

Here, $\mathcal{R}$ denotes the set of 7 asymmetry amplitudes of the unseparated fit or 14 asymmetry amplitudes of the longitudinal-to-transverse separated fit and the sum runs over the N experimental-data events. The normalization factor

$$\widetilde{\mathcal{N}}(\mathcal{R}) = \sum_{j=1}^{N_{MC}} \mathcal{W}(\mathcal{R}; \phi^j, \phi_S^j) \tag{7}$$

is determined using N_{MC} events from a PYTHIA Monte-Carlo simulation, which are generated according to an isotropic angular distribution and processed in the same way as experimental data. The number of Monte-Carlo events in the exclusive region amounts to about 40,000.

Each asymmetry amplitude is corrected for the background asymmetry according to

$$A_{corr} = \frac{A_{meas} - f_{bg} A_{bg}}{1 - f_{bg}}, \tag{8}$$

where A_{corr} is the corrected asymmetry amplitude, A_{meas} is the measured asymmetry amplitude, f_{bg} is the fraction of the SIDIS background and A_{bg} is its asymmetry amplitude. While A_{meas} is evaluated in the exclusive region, A_{bg} is obtained by extracting the asymmetry from the experimental SIDIS background in the region $2\,\text{GeV} < \Delta E < 20\,\text{GeV}$.

The systematic uncertainty is obtained by adding in quadrature two components. The first one, $\Delta A_{corr} = A_{corr} - A_{meas}$, is due to the correction by background amplitudes. In the most conservative approach adopted here, it is estimated as the difference between the asymmetry amplitudes A_{corr} and A_{meas}. This approach also covers the small uncertainty on f_{bg}. The second component accounts for effects from detector acceptance, efficiency, smearing, and misalignment. It is determined as described in Ref. [16]. An additional scale uncertainty arises because of the systematic uncertainty on the target polarization, which amounts to 8.2 %.

4 Results

The results for the five A_{UT} and two A_{UU} amplitudes, as determined in the entire kinematic region, are shown in Table 1. These results are presented in Table 3 in two intervals of Q^2 and $-t'$, with the definition of intervals together with the average values of the respective kinematic variables given in Table 2. The results for the five A_{UT} amplitudes are also shown in Fig. 5, in two rows of five panels each, where the upper and lower rows show the Q^2 and $-t'$ dependences, respectively. Each panel shows as two filled circles the results in two kinematic bins, and as one open square the result in the entire kinematic region. The results are compared to calculations of the GK model [11,21], for both signs of the $\pi\omega$ form factor. For completeness, also the model prediction without the pion–pole contribution is included.

The model predictions differ substantially upon sign change of the $\pi\omega$ form factor for the two amplitudes $A_{UT}^{\sin(\phi-\phi_S)}$ and $A_{UT}^{\sin(\phi_S)}$, in particular when considering the $-t'$ dependence. The data seem to favor a positive $\pi\omega$ transition form factor.

Asymmetry amplitudes can be written in terms of SDMEs, as shown in the "Appendix". By using Eqs. (9) and (10) and the earlier HERMES results on ω SDMEs [16],

$$A_{UU}^{\cos(\phi)} = -0.13 \pm 0.04 \pm 0.08$$
$$A_{UU}^{\cos(2\phi)} = -0.03 \pm 0.04 \pm 0.01$$

are obtained, which are consistent within uncertainties with the results shown in Table 1.

The cross section for exclusive production of transversely polarized ω mesons dominates that for longitudinally polarized ones [16]. This is the reason why the 14-parameter fit used here leads to still acceptable uncertainties for the results in the entire kinematic region on the transverse-separated asymmetry amplitudes, while those for the longitudinal-separated ones are so large that any inter-

Table 1 The amplitudes of the five sine and two cosine modulations as determined in the entire kinematic region. The first uncertainty is statistical, the second systematic. The results receive an additional 8.2 % scale uncertainty corresponding to the target polarization uncertainty

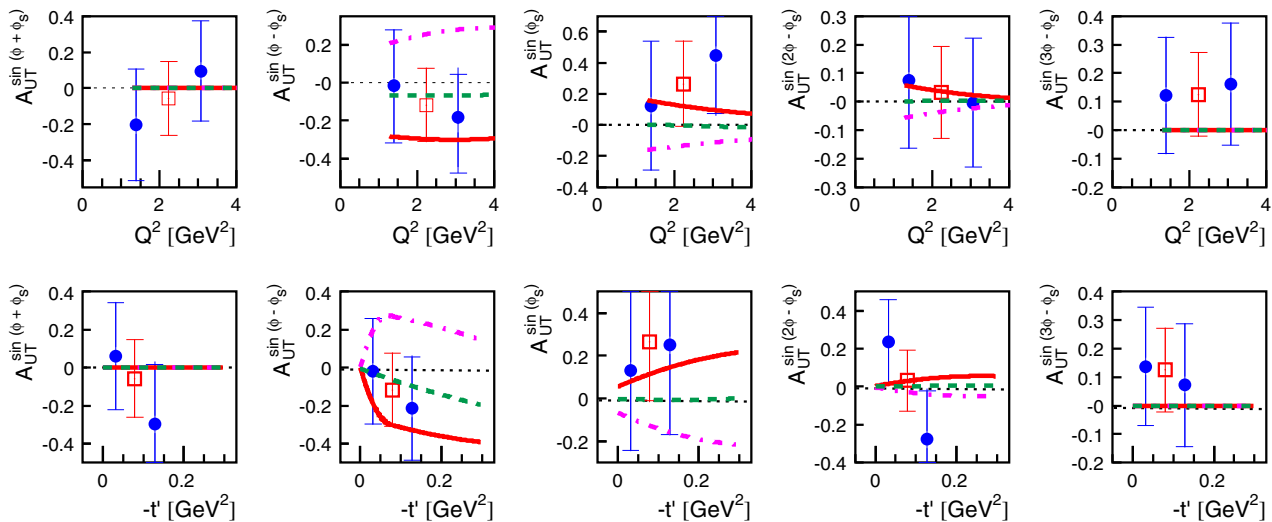| Amplitude	
$A_{UT}^{\sin(\phi+\phi_S)}$	$-0.06 \pm 0.20 \pm 0.02$
$A_{UT}^{\sin(\phi-\phi_S)}$	$-0.12 \pm 0.19 \pm 0.03$
$A_{UT}^{\sin(\phi_S)}$	$0.26 \pm 0.27 \pm 0.05$
$A_{UT}^{\sin(2\phi-\phi_S)}$	$0.03 \pm 0.16 \pm 0.01$
$A_{UT}^{\sin(3\phi-\phi_S)}$	$0.13 \pm 0.15 \pm 0.03$
$A_{UU}^{\cos(\phi)}$	$-0.01 \pm 0.11 \pm 0.10$
$A_{UU}^{\cos(2\phi)}$	$-0.17 \pm 0.11 \pm 0.05$

Table 2 The definition of intervals and the mean values of the kinematic variables

Bin	$\langle Q^2 \rangle$ [GeV^2]	$\langle -t' \rangle$ [GeV^2]	$\langle W \rangle$ [GeV]	$\langle x_B \rangle$
Entire kinematic bin	2.24	0.079	4.80	0.092
1.00 GeV$^2 < Q^2 < 1.85$ GeV^2	1.39	0.084	4.69	0.064
1.85 GeV$^2 < Q^2 < 10.00$ GeV^2	3.07	0.075	4.91	0.012
0.00 GeV$^2 < -t' < 0.07$ GeV^2	2.36	0.035	4.79	0.095
0.07 GeV$^2 < -t' < 0.20$ GeV^2	2.11	0.128	4.81	0.088

Table 3 Results on the kinematic dependences of the five asymmetry amplitudes A_{UT} and two amplitudes A_{UU}. The first two columns correspond to the $-t'$ intervals $0.00 - 0.07 - 0.20$ GeV^2 and the last two columns to the Q^2 intervals $1.00 - 1.85 - 10.00$ GeV^2. The first uncertainty is statistical, the second systematic. The results receive an additional 8.2 % scale uncertainty corresponding to the target polarization uncertainty

Amplitude	$\langle -t' \rangle = 0.035$ GeV^2	$\langle -t' \rangle = 0.128$ GeV^2	$\langle Q^2 \rangle = 1.39$ GeV^2	$\langle Q^2 \rangle = 3.07$ GeV^2
$A_{UT}^{\sin(\phi+\phi_S)}$	$0.06 \pm 0.28 \pm 0.04$	$-0.30 \pm 0.32 \pm 0.10$	$-0.21 \pm 0.31 \pm 0.05$	$0.10 \pm 0.28 \pm 0.03$
$A_{UT}^{\sin(\phi-\phi_S)}$	$-0.02 \pm 0.28 \pm 0.03$	$-0.22 \pm 0.27 \pm 0.06$	$-0.02 \pm 0.30 \pm 0.03$	$-0.18 \pm 0.26 \pm 0.03$
$A_{UT}^{\sin(\phi_S)}$	$0.13 \pm 0.37 \pm 0.03$	$0.25 \pm 0.42 \pm 0.05$	$0.12 \pm 0.42 \pm 0.02$	$0.45 \pm 0.37 \pm 0.12$
$A_{UT}^{\sin(2\phi-\phi_S)}$	$0.24 \pm 0.22 \pm 0.03$	$-0.28 \pm 0.26 \pm 0.07$	$0.07 \pm 0.24 \pm 0.02$	$-0.01 \pm 0.23 \pm 0.01$
$A_{UT}^{\sin(3\phi-\phi_S)}$	$0.14 \pm 0.21 \pm 0.01$	$0.07 \pm 0.22 \pm 0.03$	$0.12 \pm 0.20 \pm 0.04$	$0.16 \pm 0.21 \pm 0.02$
$A_{UU}^{\cos(\phi)}$	$0.05 \pm 0.15 \pm 0.06$	$-0.09 \pm 0.17 \pm 0.16$	$-0.04 \pm 0.15 \pm 0.10$	$-0.04 \pm 0.16 \pm 0.11$
$A_{UU}^{\cos(2\phi)}$	$-0.19 \pm 0.15 \pm 0.07$	$-0.14 \pm 0.17 \pm 0.07$	$-0.04 \pm 0.15 \pm 0.03$	$-0.35 \pm 0.17 \pm 0.11$

Fig. 5 The five amplitudes describing the strength of the sine modulations of the cross section for hard exclusive ω-meson production. The *full circles* show the data in two bins of Q^2 or $-t'$. The *open squares* represent the results obtained for the entire kinematic region. The *inner error bars* represent the statistical uncertainties, while the *outer ones* indicate the statistical and systematic uncertainties added in quadrature. The results receive an additional 8.2 % scale uncertainty corresponding to the target polarization uncertainty. The *solid* (*dash-dotted*) *lines* show the calculation of the GK model [11,21] for a positive (negative) $\pi\omega$ transition form factor, and the *dashed lines* are the model results without the pion pole

pretation is precluded. Also, kinematic dependences can no longer be studied due to the large uncertainties. Therefore, for the transverse-separated asymmetry amplitudes only the results in the entire kinematic region are shown in Fig. 6 and Table 4 together with the corresponding predictions of the GK model [11,21]. Here, the large uncertainties prevent any conclusion on the sign of the $\pi\omega$ transition form factor.
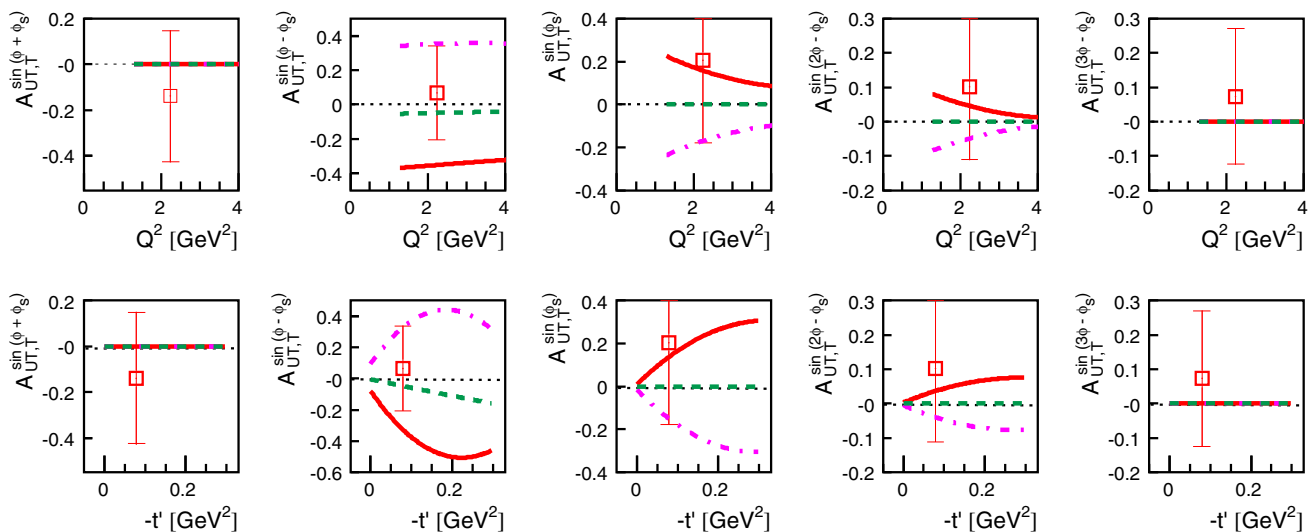
Fig. 6 As Fig. 5, but only for transversely polarized ω mesons

Table 4 Results on the five asymmetry amplitudes A_{UT} and two amplitudes A_{UU} in the entire kinematic region, but separated into longitudinal and transverse parts. The first column ($K = L$) gives the results for the longitudinal components, while the second column, ($K = T$), shows the results for the transverse components. The first uncertainty is statistical, the second systematic. The results receive an additional 8.2 % scale uncertainty corresponding to the target polarization uncertainty

Amplitude	Longitudinal ($K = L$)	Transverse ($K = T$)
$A_{UT,K}^{\sin(\phi+\phi_S)}$	$-0.16 \pm 0.92 \pm 0.02$	$-0.14 \pm 0.29 \pm 0.05$
$A_{UT,K}^{\sin(\phi-\phi_S)}$	$-0.60 \pm 0.81 \pm 0.16$	$0.07 \pm 0.27 \pm 0.04$
$A_{UT,K}^{\sin(\phi_S)}$	$-0.08 \pm 1.06 \pm 0.03$	$0.21 \pm 0.38 \pm 0.01$
$A_{UT,K}^{\sin(2\phi-\phi_S)}$	$-0.38 \pm 0.71 \pm 0.11$	$0.10 \pm 0.21 \pm 0.02$
$A_{UT,K}^{\sin(3\phi-\phi_S)}$	$0.21 \pm 0.56 \pm 0.10$	$0.07 \pm 0.20 \pm 0.01$
$A_{UU,K}^{\cos(\phi)}$	$0.53 \pm 0.40 \pm 0.08$	$-0.16 \pm 0.15 \pm 0.12$
$A_{UU,K}^{\cos(2\phi)}$	$0.60 \pm 0.39 \pm 0.17$	$-0.37 \pm 0.15 \pm 0.10$

5 Summary

In this Paper, results are reported on exclusive ω electroduction off transversely polarized protons in the kinematic region $1 \, \mathrm{GeV}^2 < Q^2 < 10 \, \mathrm{GeV}^2$ and $0.0 \, \mathrm{GeV}^2 < -t' < 0.2$ GeV^2. The amplitudes of seven azimuthal modulations of the cross section for unpolarized beam are determined, i.e., of two cosine modulations for unpolarized target and five sine modulations for transversely polarized target. Results are presented for the entire kinematic region as well as alternatively in two bins of $-t'$ or Q^2. Additionally, a separation into asymmetry amplitudes for the production of longitudinally and transversely polarized ω mesons is done. A comparison of extracted asymmetry amplitudes to recent calculations of the phenomenological model of Goloskokov and Kroll favors a positive sign of the $\pi\omega$ form factor.

Appendix: Relations between azimuthal asymmetry amplitudes and spin-density matrix elements

The full information on vector-meson leptoproduction is contained in the differential cross section $\frac{d^3\sigma}{dQ^2 dt dx}$ and the SDMEs in the Diehl representation [22]. Therefore, the azimuthal asymmetry amplitudes can be expressed in terms

of the SDMEs. For scattering off an unpolarized target, the asymmetry amplitudes can be written in terms of the Diehl SDMEs $u_{\lambda_1\lambda_2}^{\mu_1\mu_2}$ or alternatively in terms of the Schilling–Wolf SDMEs r_{ij}^n [23] as

$$
\begin{aligned}
A_{UU}^{\cos\phi} &= -2\sqrt{\epsilon(1+\epsilon)}\,\mathrm{Re}[u_{0+}] \\
&= \sqrt{2\epsilon(1+\epsilon)}\,[2r_{11}^5 + r_{00}^5],
\end{aligned}
\tag{9}
$$

$$
\begin{aligned}
A_{UU}^{\cos 2\phi} &= -\epsilon\,\mathrm{Re}[u_{-+}] \\
&= -\epsilon\,[2r_{11}^1 + r_{00}^1].
\end{aligned}
\tag{10}
$$

Here, the abbreviated notation

$$
u_{\lambda_1\lambda_2} = u_{\lambda_1\lambda_2}^{++} + u_{\lambda_1\lambda_2}^{--} + u_{\lambda_1\lambda_2}^{00}
\tag{11}
$$

is used, where λ_1, λ_2 denote the virtual-photon helicities and μ_1, μ_2 the vector-meson helicities. The symbol $\pm$ describes the virtual-photon or vector-meson helicities ± 1, while the symbol 0 describes longitudinal polarization. Equations (9) and (10) show that the asymmetry amplitudes can be calculated from the Schilling–Wolf SDMEs obtained in Ref. [16].

For scattering off a transversely polarized target, the asymmetry amplitudes can be expressed in terms of the Diehl SDMEs $n_{\lambda_1\lambda_2}^{\mu_1\mu_2}$ and $s_{\lambda_1\lambda_2}^{\mu_1\mu_2}$ as

$$
A_{UT}^{\sin(\phi+\phi_S)} = (\epsilon/2)\,\mathrm{Im}[n_{-+} - s_{-+}],
\tag{12}
$$

$$
A_{UT}^{\sin(\phi-\phi_S)} = \mathrm{Im}[n_{++} + \epsilon n_{00}],
\tag{13}
$$

$$
A_{UT}^{\sin(\phi_S)} = \sqrt{\epsilon(1+\epsilon)}\,\mathrm{Im}[n_{0+} - s_{0+}],
\tag{14}
$$

$$
A_{UT}^{\sin(2\phi-\phi_S)} = -\sqrt{\epsilon(1+\epsilon)}\,\mathrm{Im}[n_{0+} + s_{0+}],
\tag{15}
$$

$$
A_{UT}^{\sin(3\phi-\phi_S)} = -(\epsilon/2)\,\mathrm{Im}[n_{-+} + s_{-+}].
\tag{16}
$$

The abbreviated notations

$$
n_{\lambda_1\lambda_2} = n_{\lambda_1\lambda_2}^{++} + n_{\lambda_1\lambda_2}^{--} + n_{\lambda_1\lambda_2}^{00},
\tag{17}
$$

$$
s_{\lambda_1\lambda_2} = s_{\lambda_1\lambda_2}^{++} + s_{\lambda_1\lambda_2}^{--} + s_{\lambda_1\lambda_2}^{00}
\tag{18}
$$

are analogous to those in Eq. (11). In this case, Schilling–Wolf SDMEs r_{ij}^n [23] are not defined.

In order to get from Eqs. (9), (10) and (12)–(16) expressions for the asymmetry amplitudes for the production of longitudinally polarized vector mesons, the terms with $\mu_1 = \mu_2 = 0$ have to be retained in Eqs. (9)–(18), and the result has to be divided by the Schilling–Wolf SDME r_{00}^{04}. For instance, $A_{UT}^{\sin(2\phi-\phi_S)}$ becomes

$$
\begin{aligned}
A_{UT,L}^{\sin(2\phi-\phi_S)} &= -\frac{\sqrt{\epsilon(1+\epsilon)}}{r_{00}^{04}}\,\mathrm{Im}[n_{0+}^{00} + s_{0+}^{00}] \\
&= -\frac{\sqrt{\epsilon(1+\epsilon)}}{u_{++}^{00} + \epsilon u_{00}^{00}}\,\mathrm{Im}[n_{0+}^{00} + s_{0+}^{00}].
\end{aligned}
\tag{19}
$$

Correspondingly, for the production of transversely polarized vector mesons, the terms with $\mu_1 = \mu_2 = \pm 1$ have to be retained in Eqs. (9)–(18), and the result has to be divided by $(1 - r_{00}^{04})$. For instance, $A_{UT}^{\sin(2\phi-\phi_S)}$ becomes

$$
\begin{aligned}
&A_{UT,T}^{\sin(2\phi-\phi_S)} \\
&= -\frac{\sqrt{\epsilon(1+\epsilon)}}{1 - r_{00}^{04}}\,\mathrm{Im}[n_{0+}^{++} + s_{0+}^{++} + n_{0+}^{--} + s_{0+}^{--}] \\
&= -\frac{\sqrt{\epsilon(1+\epsilon)}}{1 - u_{++}^{00} - \epsilon u_{00}^{00}}\,\mathrm{Im}[n_{0+}^{++} + s_{0+}^{++} + n_{0+}^{--} + s_{0+}^{--}].
\end{aligned}
\tag{20}
$$

References

1. J.C. Collins, L. Frankfurt, M.S. Strikman, Phys. Rev. D **56**, 2982 (1997)
2. A.V. Radyushkin, Phys. Rev. D **56**, 5524 (1997)
3. X. Ji, Phys. Rev. Lett. **78**, 610 (1997)
4. M. Diehl, P. Kroll, Eur. Phys. J. C **73**, 2397 (2013)
5. P. Kroll, EPJ Web Conf. **85**, 01005 (2015)
6. S.V. Goloskokov, P. Kroll, Eur. Phys. J. C **42**, 02298 (2005)
7. S.V. Goloskokov, P. Kroll, Eur. Phys. J. C **50**, 829 (2007)
8. S.V. Goloskokov, P. Kroll, Eur. Phys. J. C **74**, 2725 (2014)
9. J. Botts, G.F. Sterman, Nucl. Phys. B **325**, 62 (1989)
10. P. Kroll, H. Moutarde, F. Sabatié, Eur. Phys. J. C **73**, 2278 (2013)
11. S.V. Goloskokov, P. Kroll, Eur. Phys. J. A **50**, 146 (2014)
12. A. Airapetian et al., HERMES Collaboration, Phys. Lett. B **679**, 100 (2009)
13. A. Airapetian et al., HERMES Collaboration, Phys. Lett. B **682**, 345 (2010)
14. A. Airapetian et al., HERMES Collaboration, JHEP **06**, 66 (2008)
15. K. Ackerstaff et al., HERMES Collaboration, Nucl. Instrum. Methods A **417**, 230 (1998)
16. A. Airapetian et al., HERMES Collaboration, Eur. Phys. J. C **74**, 3110 (2014)
17. K.A. Olive et al., Particle Data Group, Chin. Phys. C **38**, 090001 (2014)
18. T. Sjöstrand et al., Comput. Phys. Commun. **135**, 238 (2001)
19. M. Diehl, S. Sapeta, Eur. Phys. J. C **41**, 515 (2005)
20. A. Bacchetta, U. D'Alesio, M. Diehl, A.C. Miller, Phys. Rev. D **70**, 117504 (2004)
21. S.V. Goloskokov, P. Kroll, Private communication
22. M. Diehl, JHEP **09**, 064 (2007)
23. K. Schilling, G. Wolf, Nucl. Phys. B **61**, 381 (1973)